



SYNTHESIS, REPRECIPITATION METHOD AND PHARMACOLOGICAL POTENCY OF FREE PORPHYRIN BASED NANOPARTICLES

RASHA E. EL-MEKAWY^{1, 2*} AND SRAA ABU-MELHA³

¹Department of Petrochemicals, Egyptian Petroleum Research Institute, Nasr City, Cairo, Egypt

²Department of Chemistry, Faculty of applied Science, Umm Al-Qura University, Makkah Al - Mukarrama, Saudi Arabia

³Faculty of Science of Girls, King Khaled University, Abha, Saudi Arabia

ABSTRACT

We have designed and synthesized a new symmetrical porphyrins 3a-d and their nanoparticles based on extended π -conjugation concept. The new sensitizers were fully characterized by CHN analysis, UV-Vis., ¹H-NMR, TEM and Mass spectroscopy. The new sensitizers and their nanoparticles were evaluated as antitumor activity against HepG2, WI-38, VERO and MCF-7 cell lines. It was found that porphyrin nanoparticles have the most potent activity.

KEYWORDS: Pyrrole, Porphyrin, porphyrin nanoparticles, Antitumor activity



RASHA E. EL-MEKAWY

Department of Petrochemicals, Egyptian Petroleum Research Institute, Nasr City, Cairo, Egypt
Department of Chemistry, Faculty of applied Science, Umm Al-Qura University,
Makkah Al-Mukarrama, Saudi Arabia

INTRODUCTION

Nanotechnology is an emerging interdisciplinary technology that has been booming in many areas during the last decade including materials science, mechanics, electronics, optics, medicine, plastics and aerospace. Its profound societal impact has been considered as the huge momentum to usher in a second industrial revolution.^{1,2} So, the recent progress in nanoscience and nanotechnology is mainly due to the ability to synthesize, investigate and exploit materials with structural modulation in nanometer scale. Nanoparticles and/or nanocrystals in semiconductors and metals have been extensively investigated and continuously being investigated from the view point of both science and industry, e.g. thermodynamics, crystal structures, optical properties and reactivity as catalysis.^{3,4} The fabrication of the inorganic nanoparticles is generally done either by deposition methods in a molten glass matrix or by vacuum-evaporation and these processes are well developed. But these processes can not be applied conveniently for thermodynamically unstable organic compounds. Hence, preparation and characterization of stable organic nanoparticles of organic compounds of low molecular weight have not yet drawn much attention and example of organic nanoparticles are not many. Thus, effort to prepare stable and free-standing pure organic nanoparticles is indispensable. Recently much effort has been aimed at several properties of modified porphyrins nanoparticles. Porphyrins serve as a functional group in a wide variety of biological systems, the most common being chlorophyll and the heme proteins.⁵ Porphyrins, besides being helpful in understanding crucial biological processes, have enormous potential for applications including those in catalysis of organic reactions,^{6a} magnetic resonance imaging^{6b} and photodynamic therapy.^{6c} Porphyrin macrocycles are very flexible and by introducing substituents selectively at the β - or *meso*-positions, the properties can be tuned at will for any application. *meso*-Tetra arylporphyrins offer attractive features in this context and have been used in a wide variety of model systems owing to their ease of synthesis and facile functionalization. However,

the reports on porphyrins having *meso* substituents like five-membered heterocycles such as pyrrole, thiophene, furan etc are scarce.^{7, 8} In recent times, there have been a few reports on *meso*-tetrathienylporphyrins because of their unique energy transfer and electrochemical properties.⁹ In this paper, we report synthesis of porphyrin nanoparticles *via* a sonication method and will evaluate them as antitumor activity. There are only a few reports on the synthesis of porphyrin nanoparticles¹⁰⁻¹², furthermore, we acknowledge Drain *et al.*,¹³ for the strategy of preparation of porphyrin nanoparticles by a mixed solvent method.

MATERIALS AND METHODS

2.1. General remarks

All melting points are uncorrected in degree centigrade and determined on Gallenkamp electric melting point apparatus. The infrared (IR) spectra were recorded (KBr disk) on a Mattson 5000 FTIR spectrometer at the Faculty of Science, Mansoura University, Egypt. The ¹H NMR spectra were determined on a Bruker WPSY 300 MHz spectrometer with tetramethylsilane (TMS) as an internal standard and the chemical shifts are in δ ppm using dimethylsulfoxide (DMSO) as a solvent. The mass spectra were recorded at 70 eV with a Varian MAT 311 at the Microanalytical Center, Faculty of Science, Cairo University. Elemental analyses (C, H and N) were carried out at the Faculty of Science, Cairo University. The results were found to be in a good agreement (± 0.03) with the calculated values.

2.2. General procedure for the preparation of 2-(bromoalkoxy) naphthalene 1a-d

A mixture of α -naphthol and / or β -naphthol (0.72 gm, 5 mmol), dibromobutane (0.597 gm, 5 mmol) or dibromopentane (0.685 gm, 5 mmol) and anhydrous NaOH (2.2 gm, 5.5 mmol) in absolute ethanol was refluxed with stirring for 0.5-1hr at 40-60 °C until it was attained pale green to pale brown color. The reaction mixture was poured into ice water and neutralized by concentrated HCl until pH=7. The crude product was collected by filtration, washed with cold water, dried and recrystallized from ethanol to afford compounds 1a-d.

2-(4-Bromobutoxy) naphthalene (1a)

Bege cotton crystals; Yield 71 %; m.p 98 °C; IR (KBr): $\dot{\nu}/\text{cm}^{-1}$ = 3052 (Ar-CH), 2952-4752 (aliphatic CH₂), 520 (C-Br).MS: (*m/z*) 278 (M⁺, 45 %), 252 (26 %), 198 (31 %), 184 (25 %), 172 (46 %), 156 (46 %), 144 (26 %), 126 (31 %), 116 (51 %), 100 (100 %), 75 (52 %). Anal. data for C₁₄H₁₅OBr (278.03). Calcd.: C 60.23 H 5.42, Found: C 60.23 H 5.41

2-(5-Bromopentoxy) naphthalene (1b)

Bege cotton crystals; Yield; 72 %; m.p 108 °C; IR (KBr): $\dot{\nu}/\text{cm}^{-1}$ = 3050(Ar-CH), 2962 (CH₂), 480 (C-Br). MS: (*m/z*) 293 (43 %), 292 (27 %), 279 (68 %), 276 (44 %), 265 (59 %), 258 (50 %), 237 (58 %), 223 (52 %), 211 (50 %), 200 (66 %), 188 (66 %), 173 (50 %), 156 (46 %), 145 (74 %), 139 (64 %), 115 (100 %), 94 (61 %), 90 (70 %), 64 (72 %). Anal. data for C₁₅H₁₇OBr (293) Calcd.: C 61.45 H 5.84, Found: C 61.44 H 5.85

1-(4-Bromobutoxy) naphthalene (1c)

Bege cotton crystals; Yield 76 %; m.p 201 °C; IR (KBr): $\dot{\nu}/\text{cm}^{-1}$ = 3072 (Ar-CH), 2952-4752 (aliphatic CH₂), 510 (C-Br). MS: (*m/z*) 278 (M⁺, 45 %), 252 (26 %), 198 (31 %), 184 (25 %), 172 (46 %), 156 (46 %), 144 (26 %), 126 (31 %), 116 (51 %), 100 (100 %), 75 (52 %). Anal. data for C₁₄H₁₅OBr (278). Calcd.: C 60.23 H 5.42, Found: C 60.23 H 5.41

1-(5-Bromopentoxy) naphthalene (1d)

Bege cotton crystals; Yield; 62 %; m.p 168 °C; IR (KBr): $\dot{\nu}/\text{cm}^{-1}$ = 3052(Ar-CH), 2925 (CH₂), 480 (Br). Mass: (*m/z*) 293 (43 %), 292 (27 %), 279 (68 %), 276 (44 %), 265 (59 %), 258 (50 %), 237 (58 %), 223 (52 %), 211 (50 %), 200 (66 %), 188 (66 %), 173 (50 %), 156 (46 %), 145 (74 %), 139 (64 %), 115 (100 %), 94 (61 %), 90 (70 %), 64 (72 %). Anal. data for C₁₅H₁₇OBr (293) Calcd.: C 61.45 H 5.84, Found: C 61.44 H 5.85

2.3. General procedure for the preparation of phenoxyaldehydes 23a-d

A mixture of compound 1a-d (5 mile) with *p*-hydroxybenzaldehyde (0.61 gm, 5 mmol) and anhydrous NaOH (2.2 gm, 5.5 mmol) in absolute ethanol (20 ml) was refluxed with stirring for 2 hours at the 120 °C until it was attained pale brown to pale red or pink color. The reaction mixture was poured into ice water and neutralized by concentrated HCl until pH=7. The crude product was collected by filtration, washed with cold water, dried and recrystallized from ethanol to afford compound 2a-d.

4-(4-(β-naphthalene-yloxy) butoxy) benzaldehyde (2a)

Buff cotton crystals; Yield; 66 %; m.p 45.5 °C; IR (KBr): $\dot{\nu}/\text{cm}^{-1}$ = 3050 (Ar-CH), 2952-2752 (aliphatic CH₂), 1700 (CHO), 1600 (C=C), 1160 (C-O-C). ¹H-NMR (DMSO - d₆): δ/ppm = 1.75-1.88 (m, 4H, 2 CH₂), 4.10-4.17 (t, 4H, 2 OCH₂), 7.18 (d, 2H, Ar-H), 7.30 (d, 2H, Ar-H), 7.38-7.64 (m, 4H, Ar-H), 7.97 (d, 2H, Ar-H), 8.15 (d, 2H, Ar-H), 8.40 (s, 1H, Ar-H), 9.91 (s, 1H, CHO).Anal. data For C₂₁H₂₀O₃ (320). Calcd.: C 78.73 H 6.29, Found: C 78.73 H 6.29

4-(5-(β-naphthalen-yloxy)pentoxy)benzaldehyde (2b)

Buff cotton crystals; Yield; 62 %; m.p 120 °C; IR (KBr): $\dot{\nu}/\text{cm}^{-1}$ = 3052(Ar-H), 2924 (CH₂), 1697 (CHO).¹H-NMR (CDCl₃): δ/ppm = 1.60 (m, 2H, CH₂), 2.30 (m, 4H, 2 CH₂), 4.13 (t, 4H, 2 OCH₂), 7.01-7.59 (m, 11 H, A r-H), 9.58 (s, 1H, CHO). Anal. Data For C₂₂H₂₂O₃ (334) Calcd.: C 79.02 H 6.63, Found: C 79.10 H 6.62

4-(4-(α-naphthalen-yloxy)butoxy)benzaldehyde (2c)

Red cotton crystals; Yield; 66 %; m.p 120 °C; IR (KBr): $\dot{\nu}/\text{cm}^{-1}$ = 3052 (Ar-CH), 2924 (CH₂), 1697 (CHO).¹H-NMR (DMSO - d₆): δ/ppm = 1.81 (m, 2H, 2 CH₂), 4.14 (t, 2H, 2 CH₂), 7.18 (d, 2H, Ar-H), 7.28-7.53 (m, 6H, Ar-H), 7.95 (d, 2H, Ar-H), 9.91 (s, 1H, CHO). Anal. data For C₂₁H₂₀O₃ (320). Calcd.: C 78.73 H 6.29, Found: C 78.73 H 6.29

4-(5-(α-naphthalen-yloxy)pentoxy)benzaldehyde (2d)

Buff cotton crystals; Yield; 62 %; m.p 120 °C; IR (KBr): $\dot{\nu}/\text{cm}^{-1}$ = 3042(Ar-CH), 2924 (CH₂), 1687 (CHO).¹H-NMR (CDCl₃): δ/ppm = 1.62 (m, 1H, CH₂), 2.34 (m, 2H, 2 CH₂), 4.11 (t, 2H, 2 CH₂), 7.16 (d, 2H, Ar-H), 7.28-7.58 (m, 6H, Ar-H), 7.66 (d, 2H, Ar-H), 9.58 (s, 1H, CHO). Anal. data For C₂₂H₂₂O₃ (334.16). Calcd.: C 79.02 H 6.63, Found: C 79.10 H 6.62

2.4. Synthesis of porphyrin derivatives 3a-d

General Procedure: A mixture of the appropriate aromatic aldehyde (1.44 mmol), pyrrole (1.44 mmol, 0.0967 gm) in DMF (10 ml) was placed into a 100 ml three necked round-bottom flask fitted with magnetic stirrer, condenser equipped with a Dean-Stark trap, thermometer and nitrogen gas bubbler inlet tube. The reaction mixture was flushed with nitrogen gas for 5 min and then heated to 100 °C for 10 min. *p*-Toluene sulfonic acid (1.44 mmol, dissolved in 5 ml DMF) was added to the reaction mixture using a syringe. The clear, colorless reaction mixture turned various shades of red over the next 1-2 min, and was heated to 150 °C and held at this

temperature for 1 hr. Aliquots were removed from the reaction mixture to monitor it by UV-Vis. UV-Vis and DMF solutions showed the first product in the reaction to absorb at 504 nm (Q-band). On continued heating at 150 °C, the soret band of porphyrins (λ_{\max} 415-430 nm) continued to grow continuous decline in the Q band intensity. After 1 hr at 150 °C, the reaction mixture was cooled in an ice bath for 20 min. The mixture was then poured into ice-water. The precipitate was collected by filtration, dried under vacuum at ambient temperature, and the residue was purified by column chromatography (silica gel, chloroform/hexane: 1.5/1: eluent).

5,10,15,20-mesotetrakis[4-(4-(β -naphthalen-yloxy)butoxy)phenyl]-21H,23H-porphyrin (3a)

Deep reddish brown; Yield 85 %; m.p. 248 °C; IR (KBr): ν/cm^{-1} = 3409 (NH), 1612 (C=N), 1554 (C=C). ¹H-NMR(DMSO-*d*₆) δ (ppm): 1.89 (m, 16H, 8 CH₂), 2.30 (s, 1H, NH), 4.14 (t, 8H, 4 CH₂), 4.41 (t, 8H, 4 OCH₂), 5.21(d, 2H, 2 pyrrolic CH), 6.29 (d, 2H, 2 pyrrolic CH), 6.60 (d, 2H, 2 pyrrolic CH), 6.99 (d, 2H, 2 pyrrolic CH), 7.11-7.78 (m, 44H, 8 Ar-H), 10.90 (s, 1H, NH).

UV-Vis. spectrum: (λ_{\max}), 424 nm. Anal. data for C₁₀₀H₁₁₈N₄O₈ (1502). Calcd.: C 79.89 H 7.85 N 3.73, Found: C 79.90 H 7.88 N 3.74

5,10,15,20-mesotetrakis[4-(5-(β -naphthalen-yloxy)pentoxy)phenyl]-21H,23H-porphyrin (3b)

Deep red; Yield 85 %; m.p. 248 °C; IR (KBr): ν/cm^{-1} = 3409 (NH), 1612 (C=N), 1554 (C=C).

¹H-NMR(CDCl₃) δ (ppm): 1.49-1.61 (m, 16H, 8 CH₂), 1.81(m, 16H, 8 CH₂), 3.26 (s, 1H, NH), 4.06 (t, 8H, 4 OCH₂), 4.33 (t, 1H, 4 CH₂), 5.24 (d, 2H, 2 pyrrolic CH), 6.29 (d, 2H, 2 pyrrolic CH), 6.42 (d, 2H, 2 pyrrolic CH), 6.59 (d, 2H, 2 pyrrolic CH), 7.90-8.19 (d, 44H, Ar-H), 10.61 (s, 1H, NH). UV-Vis. spectrum: (λ_{\max}), 423 nm. Anal. data for C₁₀₁H₁₂₀N₄O₈ (1516).

Calcd.: C 79.94 H 7.91 N 3.69, Found: C 79.94 H 7.90 N 3.70

5,10,15,20-mesotetrakis[4-(4-(α -naphthalen-yloxy)butoxy)phenyl]-21H,23H-porphyrin (3c)

Deep reddish brown; Yield 82 %; m.p. 234 °C; IR (KBr): ν/cm^{-1} = 3349 (NH), 1622 (C=N), 1559 (C=C). ¹H-NMR(DMSO-*d*₆) δ (ppm): 1.85 (m, 16H, 8 CH₂), 2.32 (s, 1H, NH), 4.24 (t, 8H, 4 CH₂), 4.40 (t, 8H, 4 OCH₂), 5.22(d, 2H, 2 pyrrolic CH), 6.39 (d, 2H, 2 pyrrolic CH), 6.65 (d, 2H, 2 pyrrolic CH), 6.99 (d, 2H, 2 pyrrolic CH), 7.01-7.68 (m, 44H, 8 Ar-H), 10.55 (s, 1H, NH). UV-Vis. spectrum: (λ_{\max}), 425 nm. Anal. data for C₁₀₀H₁₁₈N₄O₈ (1502). Calcd.: C 79.89 H 7.85 N 3.73. Found: C 79.90 H 7.88 N 3.74

Found: C 79.90 H 7.88 N 3.74

5,10,15,20-mesotetrakis[4-(5-(β -naphthalen-yloxy)pentoxy)phenyl]-21H,23H-porphyrin (3d)

Deep red; Yield 85 %; m.p. 215 °C; IR (KBr): ν/cm^{-1} = 3400 (NH), 1632 (C=N), 1556 (C=C).

¹H-NMR(CDCl₃) δ (ppm): 1.45-1.63 (m, 16H, 8 CH₂), 1.92 (m, 16H, 8 CH₂), 3.20 (s, 1H, NH), 4.16 (t, 8H, 4 OCH₂), 4.31 (t, 1H, 4 CH₂), 5.24 (d, 2H, 2 pyrrolic CH), 6.26 (d, 2H, 2 pyrrolic CH), 6.42 (d, 2H, 2 pyrrolic CH), 6.59 (d, 2H, 2 pyrrolic CH), 7.68-8.02 (d, 44H, Ar-H), 10.41 (s, 1H, NH)

UV-Vis. spectrum: (λ_{\max}), 426 nm. Anal. data for C₁₀₁H₁₂₀N₄O₈ (1516). Calcd.: C 79.94 H 7.91 N 3.69, Found: C 79.94 H 7.90 N 3.70

2.5. Synthesis of porphyrin nanoparticles

To prepare nanoparticles we adopted 'reprecipitation method' and it is described elsewhere. In brief, first of all stock solution of said porphyrins of milliMolar concentration were prepared in dichloromethane (DCM)

(HPLC grade, Aldrich) and stored in the dark place at room temperature. Then few microliter of stock solution of porphyrin was rapidly injected into large excess of deionized water at room temperature and sonicated for 15 minutes at 50 °C. A very light yellow colloid

was obtained and used for characterization. In this research, the effect of different variables on the size of nanoparticles was examined *via* UV-vis spectroscopy.

2.6. Transmission electron microscopy (TEM)

The crystal size samples have been investigated by (TEM, Model JEM-200CX, JEOL, Japan). A few quantities of nanocomposite and copolymer were dispersed in 10 ml ethylene glycol and sonicated for 30 min. A few drops of the suspension were placed on a covered copper grid.

2.7. Pharmacology

The stock samples were diluted with RPM1-1640 medium to desired concentrations ranging from 10 to 1000 $\mu\text{g} / \text{mL}$. The final concentration of dimethylsulfoxide (DMSO) in each sample didn't exceed 1 % V / V. The activity of the synthesized compounds was tested against Vero (normal adult african green monkey cell line), WI-38 (lung fibroblast cell line), HepG2 (Hepatoma cells or Human liver hepatocarcinoma cell line), MCF-7 (Human breast adenocarcinoma cell line). The % viability of cell was examined visually. 5-Fluorouracil was used as a standard anticancer drug comparison. Briefly, cell were batch cultured for 10 d then seeded in 96 well plates of 10×10^3 cells / well in fresh complete growth medium in 96-well microtiter plastic plates at 37 °C for 24 h under 5 % CO₂ using a water jacketed carbon dioxide incubator (Shedon. TC2323. Cornelius, OR, USA). The medium (without serum) was added and cells were incubated either alone (negative control) or with different concentrations of sample to give a final concentrations of (1000, 500, 200, 100, 50, 20, 10 $\mu\text{g} / \text{mL}$). Cells were suspended in RPM1-1640 medium, 1% antibiotic-antimycotic mixture ($10^4 \mu\text{g} / \text{mL}$ potassium penicillin, $10^4 \mu\text{g} / \text{mL}$ streptomycin sulfate and 25 $\mu\text{g} / \text{mL}$ amphotericin B) and 1 % L-glutamine in 96-well flat bottom microplates at 37 °C under 5 % CO₂. After 96 hr of incubation, the medium was again aspirated, trays were inverted onto a pad of paper towels, the remaining cells rinsed carefully with medium and fixed with 3.7 % (V / V) formaldehyde in saline for at least 20 min. The fixed cells were rinsed with water and

examined. The activity was identified as confluent relatively unaltered mono-layers of stained cells treated with compounds.³⁶⁻⁴⁶

RESULTS AND DISCUSSION

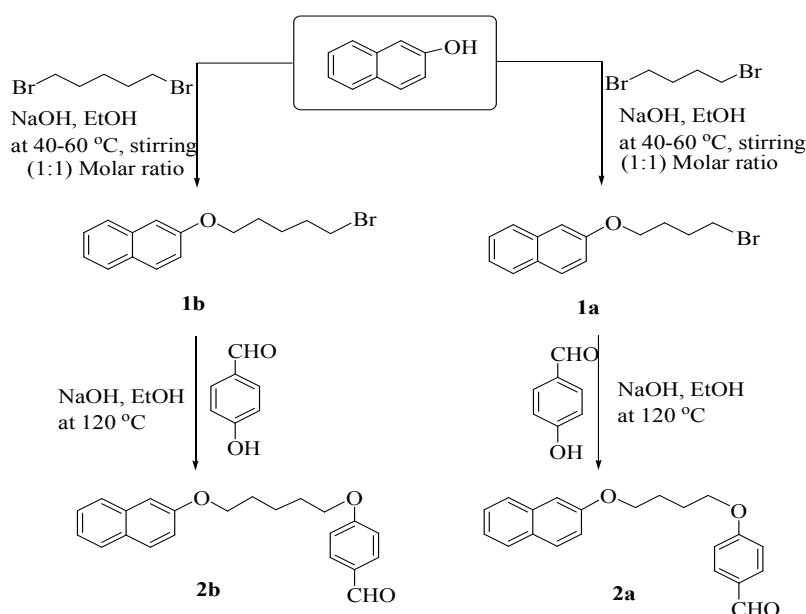
2.3. Chemistry

Porphyrins are one of the vital chemical units essential for several life processes on the earth. Many biological molecules function with prosthetic groups essentially made of these units. Because of their inherent stability, unique optical properties, and synthetic versatility, porphyrins and porphyrin nanoparticles are excellent candidates for a variety of sensing-materials applications. Research in this area has focussed on incorporation of synthetic porphyrins and porphyrin nanoparticles into a variety of material matrices, such as polymers, glasses and films. An interesting result was obtained by the synthesis of four novel porphyrin series, including the free-base compounds 3a-d which can be used as sensitizers. The main difference between them is the position of the two phenoxy butoxy group and the two phenoxy pentoxy group within the *meso*-substituted spacer, which is supposed to affect strongly the porphyrin's stereochemistry. In such cases, the contribution of the entropic factor to the system's reactivity usually proves pronounced. Hence, it seemed obvious that both the series would display a diverse biological activity. Therefore, it has been found that α - and β -naphthols were treated with 1,4-dibromobutane and/ or 1,5-dibromopentane under gentle heating with continuous stirring in ethanol in the presence of anhydrous sodium hydroxide at 40-60 °C to afford compounds 1a-d. Successfully, 1a-d were converted into 2a-d by reaction with *p*-hydroxybenzaldehyde as shown in (Scheme 1, 2). Structures 1a-d were established based on both spectral and analytical analyses. In general, the IR spectra showed absorption frequencies at ν 480-520 cm^{-1} corresponding to C-Br stretching frequencies. Structure 2a as an example was established based on its spectral analysis. The IR spectrum showed absorption frequencies at ν 1700 cm^{-1} corresponding to formyl group and 1160 cm^{-1} due to C-O-C function group. Moreover, the ¹H-NMR spectra

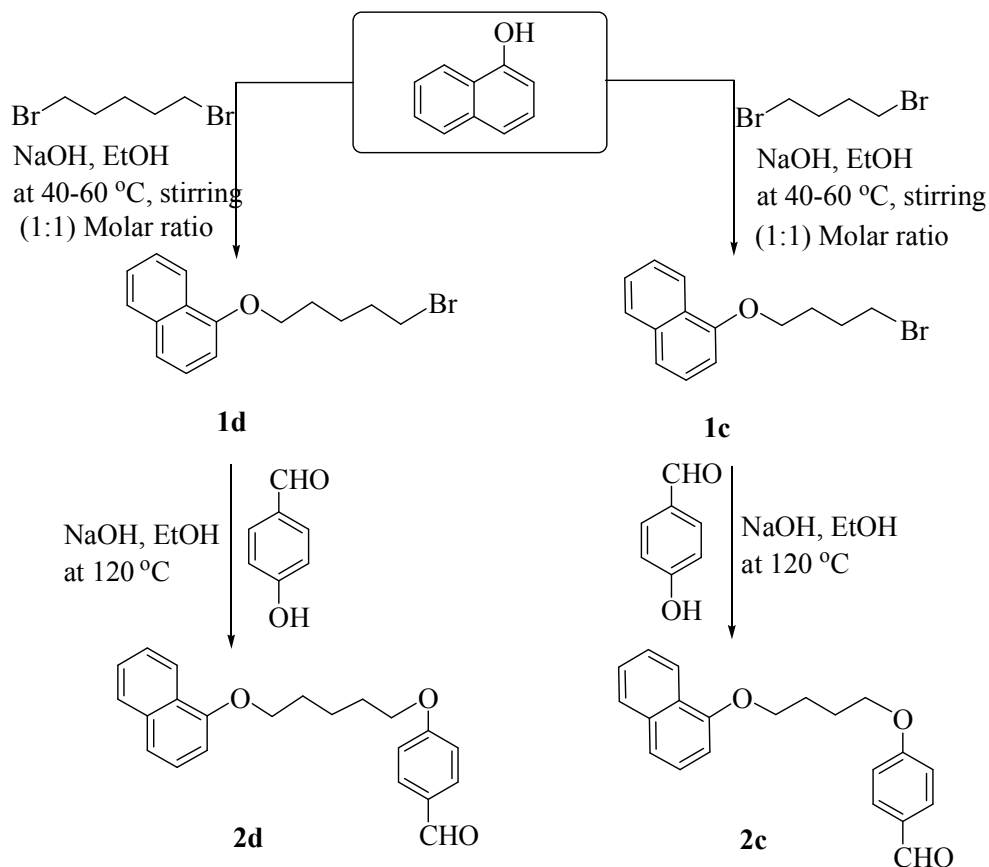
revealed characteristic multiplet signals at δ 1.75-1.88 ppm due to two CH₂ group protons, in addition to a two triplet signals at δ 4.10 and 4.17 attributable to two OCH₂ group protons, characteristic four doublet signals appeared at δ 7.10, 7.18 and 7.97, 8.15 due to two AB system and the rest of aromatic four protons appeared as multiplet signals at δ 7.32-7.59 ppm and two singlet signals at δ 8.40 and 9.91 ppm due to α -aromatic proton and formyl group proton. The IR spectrum of 2c gave a similar picture to that of 2a, while ¹H-NMR spectrum showed some differences in its

signals which showed the disappearance of AB system in naphthyl ring and the appearance of one AB system attributable to the benzaldehyde protons which appeared at δ 7.28-7.53 ppm. While compound 2d was elucidated from its correct elemental and spectral data, the IR spectrum showed absorption band at ν 2924 and 1687 cm⁻¹ corresponding to vibrational frequencies of CH₂ and CHO groups. ¹H-NMR showed a characteristic band due to two OCH₂ protons at δ 4.11 ppm as triplet signals, CHO proton appeared at δ 9.58 ppm as singlet signals.

Scheme 1
Synthesis of different aldehydes incorporating ether linkage.

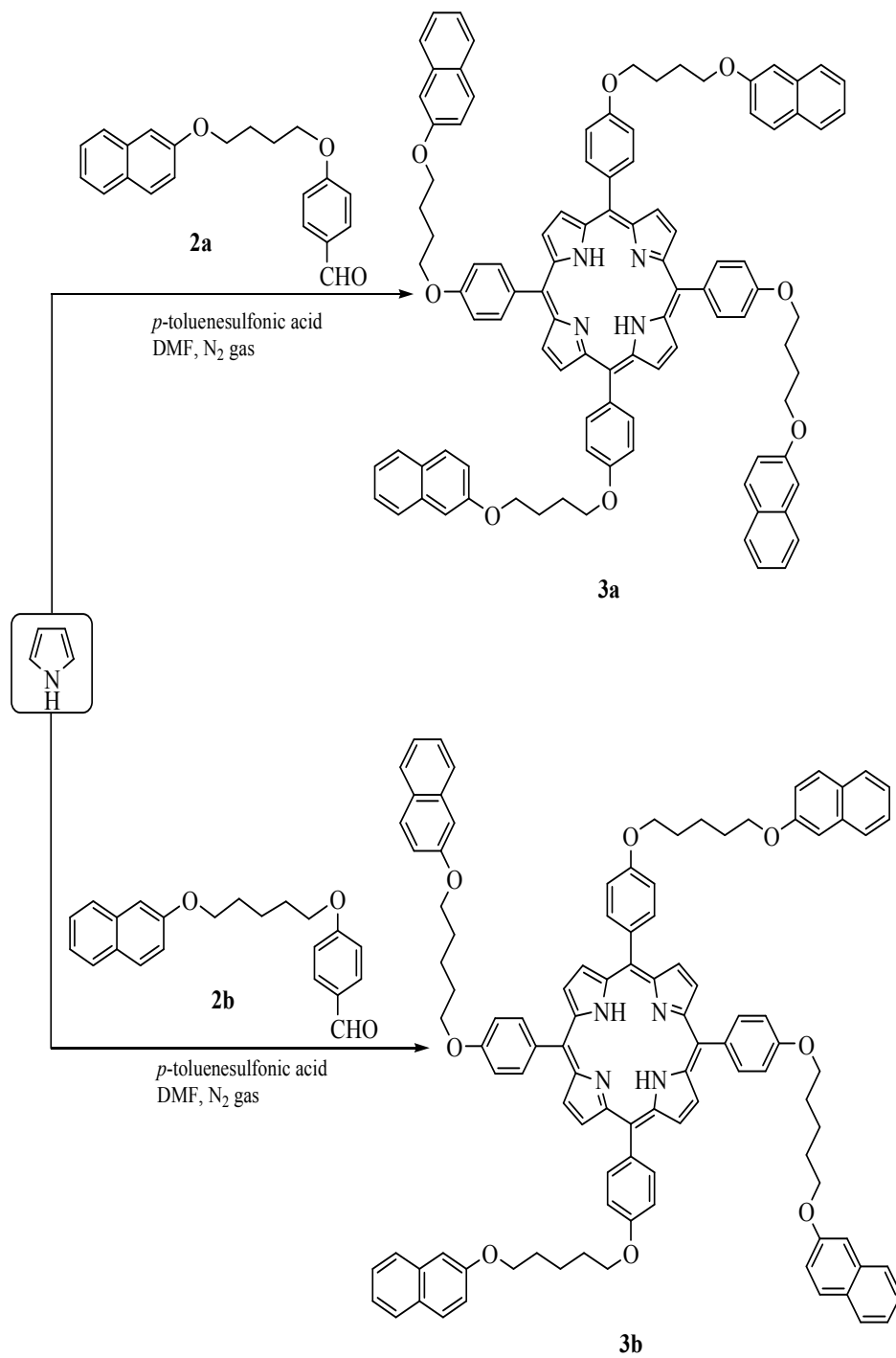


Scheme 2
Novel phenoxy aldehydes

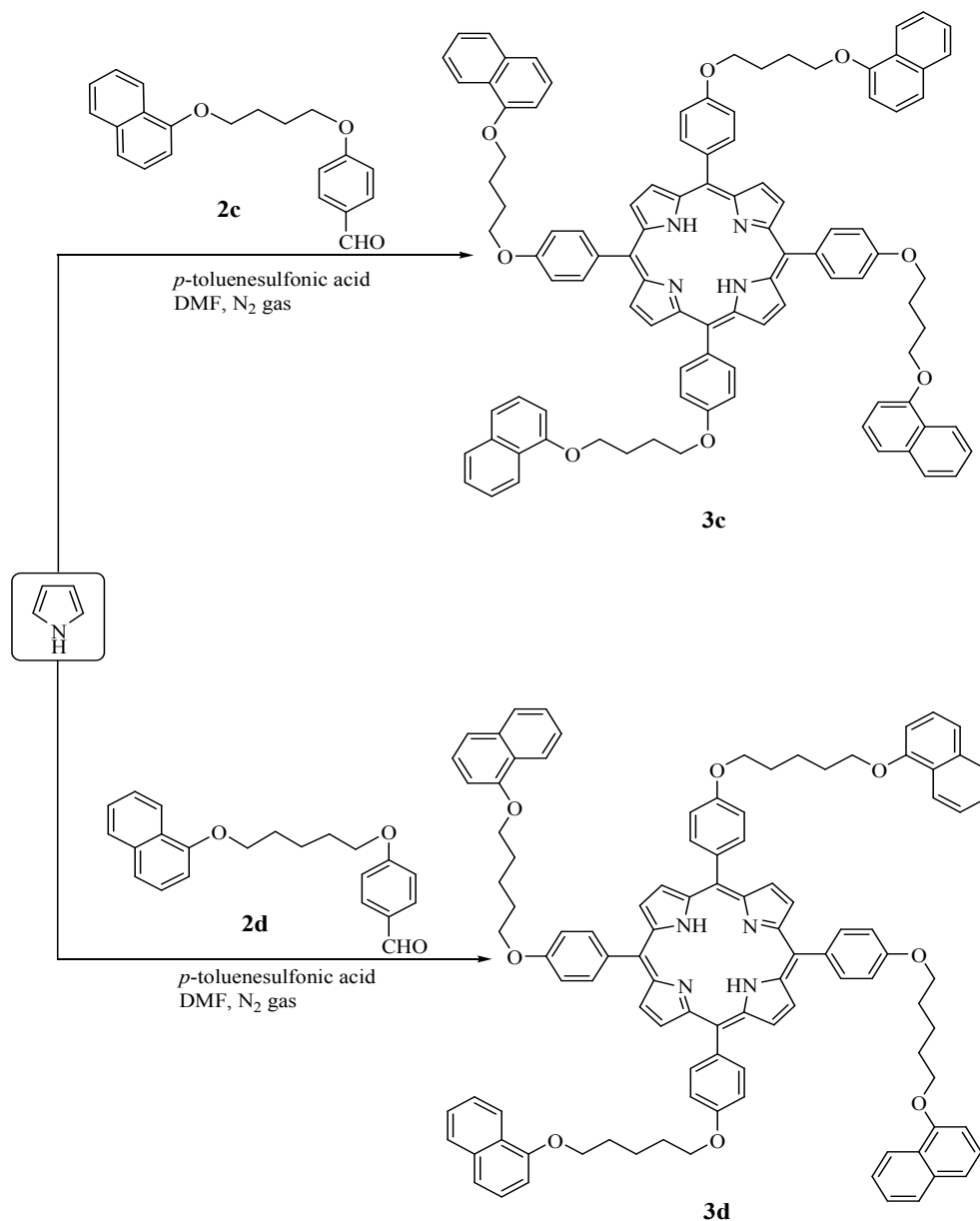


Compound 2 was successfully reacted as a starting material using different protocols of reaction in order to obtain the based porphyrins 3a-d, the based porphyrin 5,10,15,20-mesotetrakis[4-(4-(β -naphthalen-yloxy)butoxy)phenyl]-21*H*,23*H*-porphyrin (3a), 5,10,15,20-mesotetrakis[4-(5-(β -naphthalen-yloxy)pentoxy)phenyl]-21*H*,23*H*-porphyrin (3b), 5,10,15,20-mesotetrakis[4-(4-(α -naphthalen-yloxy)butoxy)phenyl]-21*H*,23*H*-porphyrin (3c), 5,10,15,20-mesotetrakis[4-(5-(α -naphthalen-yloxy)pentoxy)phenyl]-21*H*,23*H*-porphyrin (3d) were synthesized by acid-catalysed condensation of 4-(4-(β -naphthalen-yloxy)butoxy)benzaldehyde (2a), 4-(5-(β -naphthalen-yloxy)pentoxy)benzaldehyde (2b), 4-(4-(α -naphthalen-yloxy)butoxy)benzaldehyde (2c), 4-(5-(α -naphthalen-yloxy)pentoxy)benzaldehyde (2d) by statistic reaction with pyrrole in the presence of *p*-toluene sulfonic acid as acid catalyzed and as *N,N*-dimethylformamide as solvent under nitrogen gas shown in (Scheme 3, 4).

Scheme 3
Novel meso-substituted porphyrins 3a, b



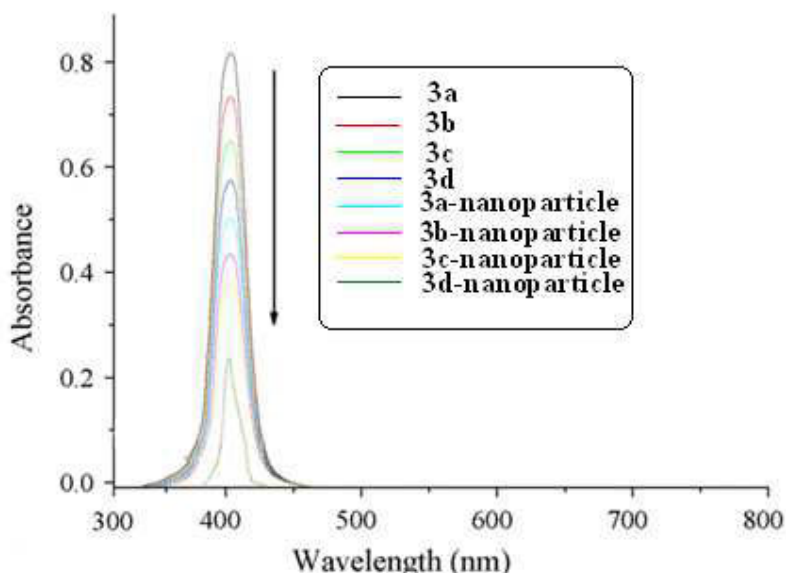
Scheme 4
Outlined scheme of new porphyrin skeletons 3c, d



Structures 3a-d were proved based on the correct analytical and spectral data. The IR spectrum in general showed absorption bands at ν 3315 cm^{-1} corresponding to NH group, 2924 cm^{-1} attributable to aliphatic CH₂, 1595 due to C=N and 1052 cm^{-1} which is a characteristic absorption band for C-O-C. ¹H-NMR spectrum (as an example) for compound 3b revealed two multiplet signals at δ 1.49-

1.61 and 1.81 ppm due to three CH₂, two triplet signals at δ 4.06 and 4.33 ppm attributable to two OCH₂ while the eight β -pyrrolic CH appeared at δ 5.24, 6.29, 6.42 and 6.59 ppm in addition to multiplet signals of 44 protons at δ 6.90-8.19 ppm. The UV-Vis spectrum of porphyrin derivatives 3a-d in general showed λ_{max} at 422-426 nm corresponding to soret band (Fig. 1).

Figure 1
UV-vis spectra of porphyrins and porphyrin nanoparticles 3a-d



Great interest in the use of porphyrin nanoparticles (PorNPs) in areas such as bionanotechnology and biomedicine is mainly due to the diverse properties presented by this kind of material, related to its size and composition. Indeed, references to the production of pure porphyrin nanoparticles are remarkably sparse in view of the few available literature on the subject. To further advance the situation, we present here the most simple and tuned process to prepare absolutely pure and discrete free-standing nanoparticles of catalytically repute 3a-d porphyrin structures. Xianchang Gong et al have claimed that they have first synthesized and characterized the porphyrin nanoparticles using mixing solvent technique but gave non pure porphyrin nanoparticles.¹⁴ Kasai et al¹⁵ different types of innovative results are being reported playing around the process.¹⁶⁻²⁵ The central idea of this process is the delicate mixture of good solvent and poor solvent of the target compound. A small volume of milli molar solution of target compound made of relatively volatile solvent is rapidly injected into a large amount of vigorously stirred poor solvent of target compound. The good solvent of target compound is miscible with poor solvent of the target compound. Hence, the good solvent is mixed with poor solvent and target compound

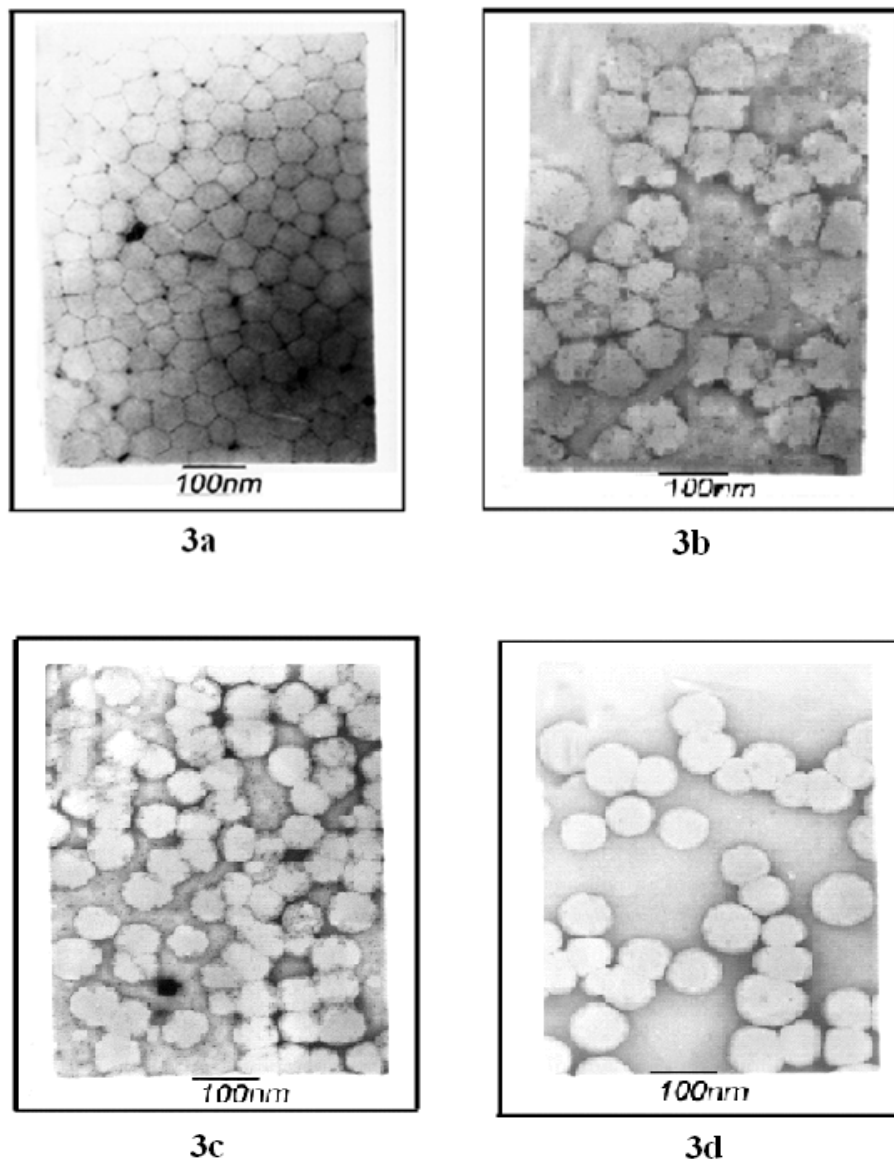
reprecipitated as nanoparticles or crystals. Herein, mechanistically we have selected DCM as good solvent. The solubility ratio of DCM in water is 1 : 100. Due to the fact, injection of 30 μ l porphyrin solution in DCM into 5 ml water will not only easily be mixed with water but also will be evaporated very fast and porphyrin will be reprecipitated as nanoparticle/crystal in water producing colloid solution of nanoparticles. The colloid solution produced by this method was found to be much stable and it was observed to sustain more than 80, 65, 52 and 45 days for 3a-d, respectively. DCM being highly volatile it could be evaporated easily even after being mixed with water leaving the produced nanoparticles dispersed in pure aqueous medium and this might have led to improve the stability of the nanoparticles. *Fig. 1* portrays the Uv-vis absorption spectra of 3a-d monomers in DCM solvent and its nanoparticles in water. Not surprisingly, the Soret band of nanoparticles is found to be composed of two extra absorption peaks at 403 and 420 nm around the monomer absorption peak at 422-426 nm indicating the existence of both *J*-type and *H*-type aggregates along with monomer in almost equal proportion. In general, porphyrins easily form aggregate through hydrophobic interaction and π - π stacking with

adjacent molecules. ²⁶⁻³⁵ Substitutions on porphyrin could lead to changing the strength of intermolecular interactions and to control the size and structures of aggregated form.

TEM was used to make comparative study between the latex particle size and morphology of the samples 3a-d.

Figure 2

TEM micrographs of the particle morphology of the porphyrin nanoparticles 3a-d samples



shows the TEM photographs of porphyrin nanoparticles, from the TEM photograph above, the particle morphology of the structures 3a-d exhibited a great change in their size than normal porphyrins. In this figure, the latex particles morphology of the sample 3d was sphericity, while the sample 3b produced a small deformation in terms of the latex particles morphology. However, the latex particles of the samples 3a and 3c showed a clear polygon-like

2.4. Antitumor activity

Cancer is a disease of striking significance in the world today. It represents the second leading cause of human mortality after cardiovascular diseases. In order to develop more effective and reliable anticancer agents, a large number of compounds bearing nitrogen-containing fused heterocyclic skeletons, have been discovered particularly and many of them exhibited excellent anticancer activity.³⁶⁻⁴⁰ Taking all of the above mentioned evidence into account, the aim of this research was to synthesize novel drugs for anticancer evaluation as a trial to obtain new antitumor agents of higher activity and lower side effects. In the present work, The selected compounds related to cyanine dye derivatives were evaluated and screened *in-vitro* as inhibitors of the growth of Vero (kidney of an African green monkey cell line), WI-38 (lung fibroblast cell line), HepG2 (Hepatoma

cells or Human liver hepatocellular carcinoma cell line) and MCF-7 (Human breast adenocarcinoma cell line) in comparison to the known anticancer drugs: 5-fluorouracil (5-Fu) and as a trial to get more effective and less toxic agent. The results were expressed in the form of the concentration of compounds that causes 50 % inhibition of cell growth. The *in vitro* evaluation revealed that some of the tested compounds revealed high inhibition activity while other compounds displayed moderate or little activity according to the obtained results outlined in Table 1. Therefore, porphyrin nanoparticles 3b and 3d have the most potent and a broad spectrum activity against HepG2, WI-38, VERO and MCF-7 cell lines. Whereas, compounds 3a and 3c have moderate activity. Finally, the rest of compounds exhibited the lowest activity.

Table 1
***In vitro* antitumor activity of tested compounds on different cell lines**

Compound No.	^a (IC ₅₀ , µg / mL)			
	HepG2	WI-38	VERO	MCF-7
3a	70.2±0.13	79.6±0.07	100±0.05	120±0.19
3b	53.4±0.12	32.3±0.13	36.3±0.24	32.5±0.03
3c	65.5±0.11	47.6±0.19	76.5±0.33	45.9±0.14
3d	33.1±0.06	39.8±0.16	42.6±0.16	29.6±0.01
3a-nanoparticle	20.02±0.01	25.3±0.21	21.9±0.08	25.6±0.23
3b-nanoparticle	18±0.11	10.3±0.13	18.1±0.19	15.9±0.18
3c-nanoparticle	24.0±0.08	21.1±0.15	15.2±0.09	18.2±0.22
3d-nanoparticle	9.2±0.15	3.7±0.31	10.3±0.19	6.1±0.06
5-Fu	8.6±0.03	3.2 ±0.01	6.5±0.04	2.3±0.02

^aIC₅₀ (mg/ mL): 1-10 (very strong), 11-25 (strong), 26-50 (moderate), 51-100 (weak), 100-200 (very weak), 200 (noncytotoxicity)

3.2.1. Structure activity relationship

From the antitumor activity results obtained for the selected porphyrin derivatives, the activity of the tested compounds could be correlated with structure variation and modification. Therefore, we noticed that all tested compounds contain diether linkage moiety showed high to moderate activity so the real effects focused on the presence of ether linkage and nanosized compounds. This is obviously clear that, PorNPs 3b and 3d showed strong activity against four different cell lines due to a long system attached to phenyl and naphthyl rings than the corresponding analogous carrying shorter linkage. The shorten of linkage system of normal porphyrin decrease the potent activity

of dyes. This variation of activity spectrum between these derivatives indicates the importance of porphyrin nanoparticles configuration which enhance physical, biological and chemical activity and thermal stability and the length of the *other linkage* system in this series of porphyrin dyes.

CONCLUSION

In conclusion, the preparation and optical characterization of porphyrin and porphyrin nanoparticlese was explained. The recorded absorption spectra show very good absorption in the UV-vis-NIR region. The pure porphyrin nanoparticles were synthesized by sonicated

method which in turn enhances the physical, chemical and biological properties and thermal stability of porphyrins 3a-d. Nanosized

compounds 3b and 3d revealed excellent potency against HepG2, WI-38, VERO and MCF-7 cell lines.

ACKNOWLEDGMENT

To Prof. Dr. Ahmed A. Fadda, Professor of Organic Chemistry, Chemistry Department, Faculty of Science, Mansoura University, Mansoura, Egypt for suggesting the point of research, his continuous guidance, precious advice, real support and valuable discussion. The authors would like to express their sincere thanks to the management of pharmacology Department, Faculty of Pharmacy, Mansoura University, for their support to carry out the antitumor activity.

REFERENCES

1. Thomas M. A big Market potential chemicals week, Nanomaterials, October 164:17-21(2002)
2. David R. Forrest, The Future impact of Molecular Nanotechnology on Textile Technology and on the textile industry, Discover Expo '95'Industrial Fabric Equipment Exposition Charlotte, North Carolina 1-16(1996)
3. Hulst H C van de. Light scattering by small particles (Dover books on physics (New York: Dover Publications Inc (December 1, 1981)
4. Murray C B, Norris D J and Bawendi M G Synthesis and characterization of nearly monodisperse CdE (E = sulfur, selenium, tellurium) semiconductor nanocrystallites. *J. Am. Chem. Soc.* 115: 8706-8715(1993)
5. Ravikanth, M.; Gupta. Fluorescence properties of meso-tetrafurlyporphyrins *J. Chem. Sci.*, 117(2):161–166 (2005)
6. (a) Meunier, B. Metalloporphyrins as versatile catalysts for oxidation reactions and oxidative DNA cleavage, *Chem. Rev.* 92:1411-1456(1992); (b) Lauffer, R. B. Paramagnetic metal complexes as water proton relaxation agents for NMR imaging: theory and design *Chem. Rev.* 87: 901-927(1987); (c) Bonnett, R. Photosensitizers of the porphyrin and phthalocyanine series for photodynamic therapy. *Chem. Soc. Rev.* 24:19-33 (1995)
7. Fadda Ahmed A, El-Mekawy Rasha E, El-Shafei Ahmed, Freeman Harold S, Hinks D, and El-Fedawy Manal, Design, Synthesis, and Pharmacological Screening of Novel Porphyrin Derivatives. *J. Chem.* 2013:1-11(2013)
8. Fadda Ahmed A, El-Mekawy Rasha E, El-Shafei Ahmed, and Freeman H. Synthesis and Pharmacological Screening of Novel meso-Substituted Porphyrin Analogs. *Arch. Pharm. Chem. Lif. Sci.* 346:53-61(2013)
9. (a) Bhyrappa P, Sankar M, Varghese B. meso-Tetrathienylporphyrins: Steady-state emission and structural properties. *J. Chem. Sci.* 118(5) 393–397(2006)
10. Gong X, Milic T, Xu C, Batteas J D, Drain C M. Preparation and Characterization of Porphyrin Nanoparticles. *J. Am. Chem. Soc.* 124: 14290–14291(2002)
11. Li X H, Xie Z H, Min H, Xian Y Z, Jin L T. Amperometric biosensor based on immobilization acetylcholinesterase on manganese porphyrin nanoparticles for detection of trichlorfon with flow-injection analysis system. *Electroanalysis*, 19:2551–2557(2007)
12. Sane A, Taylor S, Sun Y P, Thies, M.C. RESS for the preparation of fluorinated porphyrin nanoparticles. *Chem. Commun.*, 2720–2721(2003)
13. Drain C M, Smeureanu G, Patel S, Gong X, Garno J, Arijeloye J. Porphyrin nanoparticles as supramolecular systems. *New J. Chem.*, 30:1834–1843(2006)
14. Saxena V, Diaz A, Clearfield A, Batteas J D, Hussain M D. "Zirconium Phosphate Nanoplatelets: A Biocompatible Nanomaterial for Drug Delivery to Cancer," *Nanoscale* 5: 2328-2336(2013)
15. Kasai H, Nalwa H S, Oikawa H, Okada S, Matsuda H, Minami N, Kakuta A, Ono

- K, Mukoh A and Nakanishi H. A novel preparation method of organic microcrystals. *Jpn. J. Appl. Phys.* 31L (2):1132(1992)
16. Perepogu K, Bangal P R. Preparation and characterization of free-standing pure porphyrin nanoparticles. *J. Chem. Sci.* 120(5) :485-49 (2008)
 17. Drain C M, Diana S, Louis J T, Clifford E S, Efficient Microwave-Assisted Synthesis of Amine-Substituted Tetrakis(pentafluorophenyl)porphyrin. *Org. Lett.*30:1834-1843(2006)
 18. Sun W O and Young S K. Colloids and Surfaces A: Physicochemical and Engineering Aspects. 41:5257–258 (2005)
 19. Takahashi Y, Kasai H, Nakanishi H, Suzuki T M. Test strips for heavy-metal ions fabricated from nanosized dye compounds. *Angew Chem. Int. Ed.* 45(6): 913-6(2006)
 20. Gesquiere A J, Uwada T, Asahi T, Masuhara H, Barbara Paul Single Molecule Spectroscopy of Organic Dye Nanoparticles. *Nano Lett.* 5: 1321(2005)
 21. Kim H Y, Bjorklund T G, Lim S-H, Bardeen C J. Spectroscopic and Photocatalytic Properties of Organic Tetracene Nanoparticles in Aqueous Solution *Langmuir.* 19: 3941-3943(2003)
 22. Jin-Song Hu, Yu-Guo Guo, Han-Pu Liang, Li-Jun Wan and Li Jiang Facile solution synthesis of hexagonal Alq3 nanorods and their field emission properties. *J. Am. Chem. Soc.* 127: 17090(2005)
 23. Zhang X, Zhang Xiaohong, Zou Kai, Lee Chun-Sing, Lee Shuit-Tong Single-Crystal Nanoribbons, Nanotubes, and Nanowires from Intramolecular Charge-Transfer Organic Molecules. *J. Am. Chem. Soc.* 129(12): 3527 -3532(2007)
 24. Fu H B and Yao J N. Size Effects on the Optical Properties of Organic Nanoparticles. *J. Am. Chem. Soc.* 123(7): 1434-1439(2001)
 25. Al-Kaysi R O, Muller A M, Ahn Tai-Sang, Lee S, Bardeen C J. Effects of Sonication on the Size and Crystallinity of Stable Zwitterionic Organic Nanoparticles Formed by Reprecipitation in Water. *Langmuir.* 21(17): 7990-7994(2005)
 26. Li L L, Yang C J, Chen W H and Lin K J Towards the Development of Electrical Conduction and Lithium-Ion Transport in a Tetragonal Porphyrin Wire. *Angew. Chem. Ind. Ed.* 42(13):1505-1508(2003)
 27. Lin K J. SMTP-1: The First Functionalized Metalloporphyrin Molecular Sieves with Large Channels. *Angew. Chem. Ind. Ed.* 38(18): 2730-2732(1999)
 28. Diskin-Posner Y, Dahal S, Golberg I. Crystal Engineering of Metalloporphyrin Zeolite Analogues. *Angew.Chem. Ind. Ed.* 112(7):1344-1348(2000)
 29. Li G, Fudickar W, Skupin M, Klyszcz A, Draeger C, Lauer M, Fuhrhop J H. Rigid lipid membranes and nanometer clefts: motifs for the creation of molecular landscapes. *Angew. Chem. Ind. Ed.* 41: 1828-1831(2002)
 30. Doon S C, Shanmughan S, Aston D E, Mettal J L. Counterion Dependent Dye Aggregates: Nanorods and Nanorings of Tetra(*p*-carboxyphenyl)porphyrin. *J. Am. Chem. Soc.* 127(16): 5885-5892(2005)
 31. Koti A S, Periasamy R N. Cyanine induced aggregation in *meso*-tetrakis(4-sulfonatophenyl)porphyrin anions. *J. Mater. Chem.*12: 2312-1317(2002)
 32. Van der Boom T, Hayes R T, Zahao Y, Bushard P J, Weiss E A, Wasielewski M R. Charge Transport in Photofunctional Nanoparticles Self-Assembled from Zinc 5,10,15,20-Tetrakis(perylene-diimide)porphyrin Building Blocks. *J. Am. Chem. Soc.* 124(132):9582-95890(2002)
 33. Tsuda A, Sakamoto S, Yamaguchi K, Aida T. A Novel Supramolecular Multicolor Thermometer by Self-Assembly of a π -Extended Zinc Porphyrin Complex. *J. Am. Chem. Soc.* 125(51):15722-15723(2003)
 34. Balaban T S, Goddard R, Linke-Schaetzl M, Leng J M. 2-Aminopyrimidine Directed Self-Assembly of Zinc Porphyrins Containing Bulky 3,5-Di-tert-butylphenyl Groups. *J. Am. Chem. Soc.* 125(14): 4233-4239(2003)
 35. Takahashi R, Kobuke Y J. Hexameric Macroring of Gable-Porphyrins as a Light-Harvesting Antenna Mimic. *J. Am. Chem. Soc.* 125(9):2372-2373(2003)

36. Zhai X, Zhao YF, Liu YJ, Zhang Y, Xun FQ, Liu J, Gong P. Synthesis and Cytotoxicity Studies of Novel [1,2,4]Triazolo[1,5-a]pyrimidine-7-amines. *Chem. Pharm. Bull.* 56(7): 941-945(2008)
37. Gupta A, Priya N, Jalal S, Singh P, Chand K, Raj HG, Parmar VS, et al. Specificity of Calreticulin Transacetylase to acetoxy derivatives of benzofurans: Effect on the activation of platelet Nitric Oxide Synthase. *Biochimie*; 92(9): 1180-1185 (2010).
38. Abdel-Aziz H, Abdel-Wahab B, Badria F. Stereoselective Synthesis and Antiviral Activity of (1*E*,2*Z*,3*E*)-1-(Piperidin-1-yl)-1-(arylhydrazono)-2-[(benzoyl/benzothiazol-2-yl)hydrazono]-4-(aryl¹)but-3-enes. *Arch. der Pharm.* 343(3): 152-9(2010)
39. Mohamed HA, Dawood K, Badria F. Cytotoxicity and Utility of 1-Indanone in the Synthesis of Some New Heterocycles. *Chem. Pharm. Bull.* 58 (4): 479-483(2010)
40. Ayyad SN, Ezmirly ST, Basaif SA, Alarif WM, Badria AF. Antioxidant, cytotoxic, antitumor, and protective DNA damage metabolites from the red sea brown alga *Sargassum* sp. *Pharmacology research.* 3(3): 160-5(2011)
41. Abdel-Wahab BF, Awad GEA, Badria FA. Synthesis, antimicrobial, antioxidant, anti-hemolytic and cytotoxic evaluation of new imidazole-based heterocycles. *Euro. j.med. chem.*46(5): 1505-11(2011)
42. Ayyad SN, Makki MS, Al-Kayal NS, Basaif SA, El-Foty KO, Asiri AM, Alarif WM, Badria FA. Cytotoxic and protective DNA damage of three new diterpenoids from the brown alga *Dictyota dichotoma*. *Euro. j. med. Chem.* 46(1): 175-82(2011)
43. Badr AE, Omar N, Badria FA. A laboratory evaluation of the antibacterial and cytotoxic effect of Liquorice when used as root canal medicament. *Int. endo. J.* 44(1): 51-8(2011)
44. Abdelhafez OM, Abdelatif NA, Badria FA. NA binding, antiviral activities and cytotoxicity of new furochromone and benzofuran derivatives. *Arch. Pharmacol research.* 34(10):1623-32(2011)
45. Bondock S, Adel S, Etman HA, Badria F A. Synthesis and antitumor evaluation of some new 1,3,4-oxadiazole-based heterocycles. *Euro. j.med. chem.* 48:192-9 (2012)
46. Ayyad SN, Abdel-Lateff A, Alarif WM, Patacchioli FR, Badria FA, Ezmirly ST. *In vitro* and *in vivo* study of cucurbitacins-type triterpene glucoside from *Citrullus colocynthis* growing in Saudi Arabia against hepatocellular carcinoma. *Environ. Toxicol. Pharmacol.* 33(2):245-251(2012)